Proceedings of the 21st ICSMGE, Vienna, Austria, 14 – 19 June 2026. Pistrol, Adam & Schweiger (eds.)
Published by: ÖGG, Austrian Society for Geomechanics, Salzburg, Austria, ISBN 978-3-9503898-4-5
https://doi.org/10.53243/ICSMGE2026-831

Artificial ground freezing under high-velocity seepage

Petr Nikolaev
Department of Earth Science and Engineering, Imperial College London, United Kingdom, p.nikolaev@imperial.ac.uk
School of Engineering, The University of Manchester, United Kingdom

Andrey P. Jivkov, Majid Sedighi
School of Engineering, The University of Manchester, United Kingdom

ABSTRACT: Artificial ground freezing (AGF) is a well-established ground improvement technique used to provide the safety of underground construction in water-bearing soils. The method temporarily freezes the soil around the construction zone, increasing its strength and rendering it impermeable to water flow. However, the formation of a ground-ice cofferdam can be significantly hindered by high-velocity groundwater flow, a condition commonly encountered in coarse-grained soils due to their high hydraulic conductivity. This challenge can be addressed by employing expendable refrigerants such as solid carbon dioxide or liquid nitrogen, which enables lower freezing temperatures compared to the conventional systems that rely on electrically powered plants and cooled secondary fluids (e.g., brine). To ensure an appropriate choice of freezing method and cost-effective implementation under given geological conditions, accurate prediction of ice-wall formation is essential. This study introduces a novel Peridynamics-based model for analysing and designing ground freezing in high-velocity seepage conditions. The non-local (spatially integral) formulation provides a more stable solution to the convection-dominated heat transfer problem, while effectively capturing abrupt changes in the thermophysical properties of soils during phase-change front propagation - an area where conventional local (differential) methods often struggle. The proposed approach yields reliable insights into the influence of key geological and technological parameters on ice-wall development, supporting the broader application of AGF in engineering projects worldwide.

KEYWORDS: Artificial ground freezing, peridynamics, phase change, couple modelling, ground water flow.

1 INTRODUCTION

Artificial ground freezing (AGF) is a technique for temporary ground improvement in construction and mining, particularly effective for groundwater control and structural support (Harris, 1995; Andersland and Ladanyi, 2004). Among its applications, the use of expendable refrigerants such as liquid nitrogen (LN) and solid carbon dioxide (SCD) has attracted increasing attention because of their ability to rapidly form ice walls in high-permeability soils (Nikolaev et al., 2022b).

Modelling AGF presents significant challenges due to the complex and coupled thermal and hydraulic processes involved, especially under high-velocity groundwater flow. In such conditions, convective heat transfer is the dominant regime, often preventing stable ice wall formation. Although a range of analytical and numerical models has been developed (Alzoubi et al., 2020), most employ local formulations such as the finite element method (FEM). These approaches frequently suffer from numerical instabilities in convection-dominated regimes and have difficulty capturing sharp phase transitions in soils.

Peridynamics (PD), a non-local, mesh-free computational framework, provides a promising alternative. By reformulating governing equations in integral form, PD effectively handles discontinuities and strong nonlinearities (Madenci and Oterkus, 2014). Originally developed for solid mechanics, PD has since been extended to thermal and multi-physics problems, including ground freezing with phase change (Nikolaev et al., 2022a; 2024). This paper presents a bond-based peridynamic model for simulating AGF under groundwater flow conditions. The model is applied to assess the effectiveness of expendable refrigerants in supporting ice wall formation across a range of geological and operational scenarios.

2 PERIDYNAMIC DESCRITION OF THE GROUND-ICE WALL FORMATION

The formation of a ground-ice wall is predicted using the peridynamic (PD) model developed by Nikolaev et al. (2024; 2025). In this approach, the soil volume is represented as an assembly of individual particles, illustrated in Fig. 1. Each particle has a square shape defined by its characteristic size $\Delta_x(\mathbf{x})$ and is identified by a position vector $\mathbf{x}$ relative to a fixed Cartesian coordinate system. A particle located at position $\mathbf{x}$ interacts with all particles at positions $\mathbf{x}'$ within a defined spatial region $\mathcal{H}_x$ known as its horizon. Formally, the horizon of a particle $\mathbf{x}$ is $\mathcal{H}_x = \{\mathbf{x}' : |\mathbf{x}' - \mathbf{x}| \leq \delta\}$, where the constant δ denotes the horizon radius. Interactions between two particles at positions $\mathbf{x}$ and $\mathbf{x}' \in \mathcal{H}_x$ are termed t-bonds (transport bonds). The distance vector between these particles is $\boldsymbol{\xi} = (\mathbf{x}' - \mathbf{x})$.

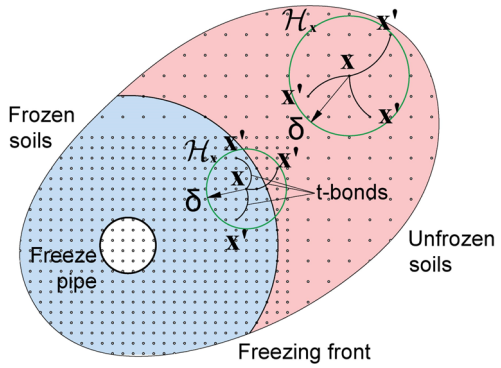

Figure 1. Peridynamics domain discretization (Nikolaev et al., 2024)

Following Nikolaev et al. (2024), the soil volume is divided into two regions: frozen region, where pores are filled with ice, and unfrozen region, where ice is absent. These regions are separated by an interface at temperature T_f. In this framework, the enthalpy-based energy conservation equation, incorporating both heat conduction and advective transport, is employed:

$$\frac{\partial \mathrm{H}(x,t)}{\partial \mathrm{t}} = \int_{\mathcal{H}_x} \left[\Lambda(\mathbf{x}', \mathbf{x}, t) \frac{T(\mathbf{x}', t) - T(\mathbf{x}, t)}{||\xi||^2} - \rho_w C_w U(\mathbf{x}', \mathbf{x}, t) \frac{T(\mathbf{x}', t) - T(\mathbf{x}, t)}{||\xi||} \right] \mathrm{d}V_{\mathbf{x}'} \quad (1)$$

Here, $H(x,t)$ and $T(x,t)$ denote the enthalpy and the tempeature of a soil PD particle, respectively; ρ and C represent density and the specific heat capacity; t is time; $\Lambda(x',x,t)$ is the PD microscopic thermal conductivity, and $U(\boldsymbol{x}',\boldsymbol{x},t)$ is PD microscopic groundwater flow velocity. Parameters with subscripts s, w, and i correspond to the soil particles (matrix), liquid water, and solid water (ice), respectively. Subscripts f and un, denote frozen and unfrozen states, respectively.

The PD thermal micro-conductivity and water micro-velocity for two-dimensional domains are defined as:

$$\Lambda(\mathbf{x}',\mathbf{x},t)=\frac{4\overline{\lambda}(\mathbf{x}',\mathbf{x},t)}{\pi\delta^2},U(\mathbf{x}',\mathbf{x},t)=\frac{2\overline{u}(\mathbf{x}',\mathbf{x},t)}{\pi\delta^2} \quad (2)$$

where $\overline{\lambda}(\mathbf{x}',\mathbf{x},t)=[\lambda(\mathbf{x},t)+\lambda(\mathbf{x}',t)]/2$ is the average thermal conductivity of soil particles connected by a single t-bond, and $\overline{u}(\mathbf{x}',\mathbf{x},t)=[u(\mathbf{x},t)+u(\mathbf{x}',t)]/2$ is the average water velocity through such particles.

Given a particle's enthalpy, its temperature and phase state are determined as:

$$T(\mathbf{x},t)=\begin{cases}\dfrac{H(\mathbf{x},t)}{\rho_f C_f}, & \text{frozen soils}\\ \dfrac{H(\mathbf{x},t)-(\rho_f C_f T_f+\rho_f \Pi L)}{\rho_{un}C_{un}}, & \text{unfrozen soils}\end{cases} \quad (3)$$

where L_w is the specific latent heat of solidification of water and Π denotes the soil porosity. If $T(\mathbf{x},t)\le T_f$, the particle is considered frozen and belongs to the frozen region; otherwise it remains unfrozen.

The average volumetric heat capacity of saturated frozen and unfrozen soil PD particles is:

$$\begin{aligned}\rho_f C_f(\mathbf{x},t)&=\rho_i C_i\Pi(1-S_{w,res})+\rho_w C_w\Pi_w\\&\quad+\rho_s C_s(1-\Pi),\\ \rho_{un}C_{un}(\mathbf{x},t)&=\rho_w C_w\Pi+\rho_s C_s(1-\Pi)\end{aligned} \quad (4)$$

where $S_{w,res}$ is the residual water content.

The average thermal conductivity of a soil PD particle is:

$$\begin{aligned}\lambda_f(\mathbf{x},t)&=\lambda_i^{\Pi(1-S_{w,res})}\lambda_w^{\Pi S_{w,res}}\lambda_s^{(1-\Pi)},\\ \lambda_{un}(\mathbf{x},t)&=\lambda_w^{\Pi}\lambda_s^{(1-\Pi)}\end{aligned} \quad (5)$$

For particles with $T(\mathbf{x},t)=T_f$, the thermal conductivity is taken as $[\lambda_f(\mathbf{x},t)+\lambda_{un}(\mathbf{x},t)]/2$.

The volume of liquid water in frozen soils at a given subzero temperature is determined solely by the change in particle's enthalpy: $S_w(\mathbf{x},t)=0$ for the frozen soil, and $S_w(\mathbf{x},t)=1$ for unfrozen soil. Enthalpy values at T_f are linearly interpolated.

The peridynamic formulation of pore-water mass conservation, following Nikolaev et al. (2024), is:

$$\begin{aligned}&\Pi\frac{(\rho_w-\rho_i)}{\rho_w}\frac{\partial S_w(\mathbf{x},t)}{\partial t}\\&=\int_{\mathcal{H}_x}K_w(\mathbf{x}',\mathbf{x},t)\frac{\Phi(\mathbf{x}',t)-\Phi(\mathbf{x},t)}{\|\xi\|^2}\,\mathrm{d}V_{\mathbf{x}'}\end{aligned} \quad (6)$$

where, $S(\mathbf{x},t)$ is the saturation degree ($S_w+S_i=1$); $u(\mathbf{x},t)$ is the water flux; $\Phi(\mathbf{x},t)$ is the flow potential; and $K_w(\mathbf{x}',\mathbf{x},t)$ is the PD micro-permability of a single t-bond. For two-dimensional problems, the PD micro-permeability under uniform constant influence functions is:

$$K_w(\mathbf{x}',\mathbf{x},t)=\frac{4k_{int}\overline{k_r}(\mathbf{x}',\mathbf{x},t)}{\mu\pi\delta^2} \quad (7)$$

where $\overline{k_r}(\mathbf{x}',\mathbf{x},t)=[k_r(\mathbf{x}',t)+k_r(\mathbf{x},t)]/2$ is the relative permeability of the t-bond; k_{int} is the intrinsic permeability of the porous medium; and μ is the dynamic viscosity of liquid water.

In the frozen region, the relative permeability is zero, while in the unfrozen zone it equals one. For particles at $T(\mathbf{x},t)=T_f$, the relative permeability is assumed equal to the relative water content $S_w(\mathbf{x},t)$.

Given the known water potential field, the water flux at any PD particle $\mathbf{x}$ is:

$$\begin{aligned}&u(\mathbf{x},t)\\&=\int_{\mathcal{H}_x^+}K_w(\mathbf{x}',\mathbf{x},t)\frac{\Phi(\mathbf{x}',t)-\Phi(\mathbf{x},t)}{\|\xi\|}\frac{\xi}{\|\xi\|}\,\mathrm{d}V_{x'}\end{aligned} \quad (8)$$

where $\mathcal{H}_x^+$ denotes the portion of the horizon of $\mathbf{x}$ encompassing particles with higher potential than $\Phi(\mathbf{x},t)$.

Further details of the numerical implementation, boundary conditions, and modelling assumptions are provided in (Nikolaev et al., 2024).

3 ANALYSIS OF ICE-WALL FORMATION

This section presents the results of a comprehensive parametric study designed to evaluate the influence of technological factors on the dynamics of linear ice wall formation. The computational domain is presented in Fig. 2. For more details on the results under consideration, see Nikolaev et al. (2024; 2025).

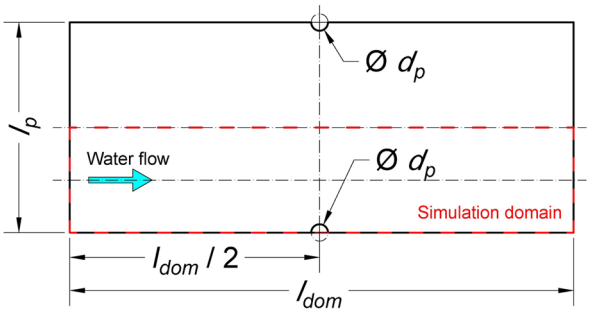

Figure 2. The geometrical domain of the parametric study

3.1 *Geological and thermophysical conditions*

The analysis is performed for a representative coarse-grained soil with the following thermophysical properties: solid matrix density - 2650 kg/m³; specific heat capacity - 835 J/(kg °C); thermal conductivity - 3 W/(m °C); intrinsic permeability - $1.8\cdot10^{-11}$ m²; porosity - 0.5; initial soil temperature - 7 °C.

Three freeze-pipe spacings are considered: 0.96 m, 1.20 m, and 1.44 m. Pipe diameters of 0.10 m, 0.125 m, and 0.15 m are analysed.

3.2 *Ground freezing methods*

Three freezing methods are studied: Brine freezing with pipe temperature −25 °C; Solid carbon dioxide (SCD) freezing with pipe temperature −70 °C; and Liquid nitrogen (LN) freezing with pipe temperature −120 °C

The critical seepage velocities at which ice walls can still be formed, along with the corresponding freezing times, $t_{f,cr}$, are presented in Fig. 3.

Simulation results indicate that conventional brine freezing can form a continuous ice wall only under low seepage conditions (≤0.3 m/day). In contrast, SCD freezing enables

wall formation at seepage rates up to ~2 m/day, while LN freezing remains effective at rates up to ~3.8 m/day. Thus, ice wall formation remains achievable up to a critical seepage value, beyond which freezing becomes unfeasible.

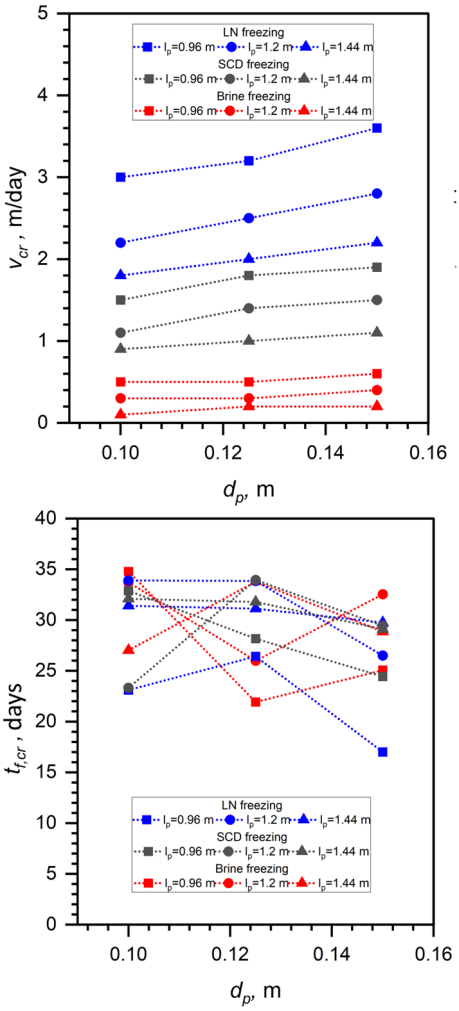

Figure 3. The critical v_{cr} seepage values and corresponding to them critical $t_{f,cr}$ freezing time

The freezing time, $t_{f,cr}$, required at critical seepage conditions remains relatively consistent across methods, ranging between 25 and 35 days. If an ice wall has not formed within this timeframe, further freezing is highly unlikely. However, the use of expendable refrigerants (SCD and LN) over extended periods may be impractical due to sharply increased consumption. For example, with LN freezing (pipe diameter 0.125 m and spacing 1.20 m), increasing groundwater velocity from 0 to 2.4 m/day leads to a near-linear rise in freezing time from 2.14 to 7.32 days. A further increase to 3.0 m/day causes a sharp jump to 23.1 days. Thus, freezing should not be attempted when seepage approaches the critical velocity v_{cr}.

To address this, the concept of an *allowable freezing velocity* is introduced, defined as the maximum seepage velocity for which freezing time increases approximately linearly with seepage. Exceeding this threshold results in disproportionately large freezing times. Such a velocity cannot be defined for brine freezing. Based on the results, the allowable seepage should be defined such that $v_{al}^{\mathrm{LN}} \approx 0.8 v_{cr}$ for LN freezing and $v_{al}^{\mathrm{SCD}} \approx 0.7 v_{cr}$ for SCD freezing.

For geological conditions where several freezing methods are feasible, the choice should be based on an economic comparison (Nikolaev et al. 2025). For relatively small volumes of frozen soil, typically less than 200 to 1000 m³, the cost of SCD freezing is lower than that of brine systems because it does not require a refrigeration plant or a coolant distribution network. SCD freezing also requires a smaller quantity of refrigerant than LN freezing for the same frozen volume, which makes the method more attractive. Although the LN method delivers the ice wall more quickly, the overall construction time may be similar or even shorter with the SCD approach once the considerably longer installation time of an LN freezing plant is considered. The SCD method may become impractical for large scale applications, since it requires manual loading of substantial quantities of refrigerant into the pipes, which considerably increases labour demand.

3.3 *Diameter of the freeze pipes*

Freeze pipe diameter strongly influences both critical seepage, v_{cr}, and freezing time, t_f, as it controls the total heat flux extracted. As shown in Fig. 3, increasing d_p from 0.10 m to 0.125 m raises v_{cr} by ~10%, while an increase to 0.15 m yields ~20% higher v_{cr}, regardless of freezing method or pipe spacing.

The effect on freezing time t_f is more complex. Figure 4 compares freezing times for 0.125 m and 0.15 m pipes relative to 0.10 m pipes. Without seepage, increasing diameter from 0.10 m to 0.125 m reduces freezing time by ~10%, while an increase to 0.15 m reduces it by ~20%. Depending on pipe spacing and freezing method, reductions of up to 40–70% are possible under seepage conditions. Nevertheless, in cases of relatively low seepage, smaller pipe diameters may be more cost-effective due to reduced drilling costs.

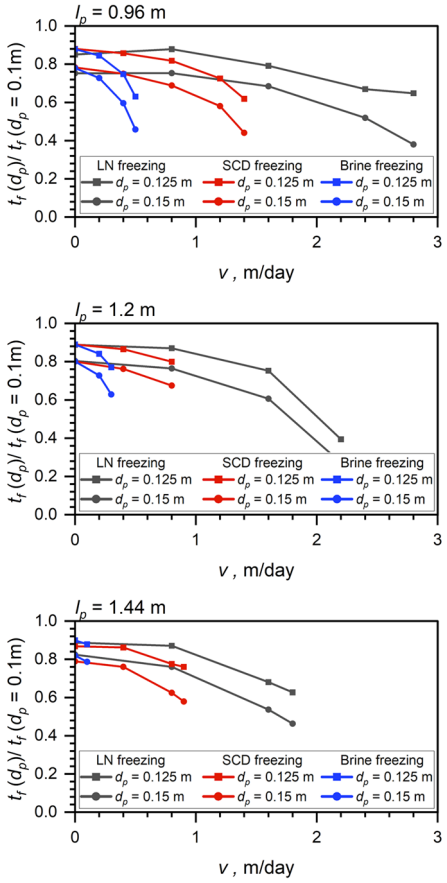

Figure 4. The relative time t_f that is required to create the ice wall by the freeze pipes with diameters of 0.125 m and 0.15 m compared to the time of the ice wall formation by application of the freeze pipe with the diameter of 0.1 m

3.4 *Distance between freeze pipes*

Pipe spacing controls the number of freeze pipes required, and thus directly affects installation costs. Optimizing spacing is therefore essential for cost-effective ice wall formation. As shown in Fig. 3, spacing strongly affects freezing time, particularly at higher groundwater velocities. Excessive spacing may prevent wall formation altogether.

Figure 5 compares freezing times for spacings of 1.20 m and 1.44 m relative to 0.96 m. Without seepage, increasing spacing from 0.96 m to 1.20 m lengthens freezing time by ~1.5×, while a further increase to 1.44 m triples the required time. This pattern is consistent across freezing methods and pipe diameters.

The analysis indicates that larger spacings are feasible only when using expendable refrigerants (LN or SCD). For brine freezing, shorter spacings are advisable even under low seepage, to ensure reliable ice wall delivery.

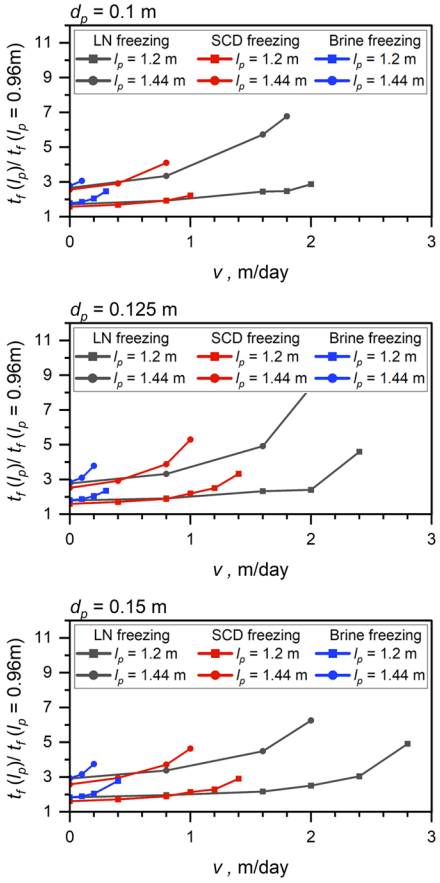

Figure 5. The relative time t_f that is required to create the ice wall with the distance between the freeze pipes of 1.2 m and 1.44 m compared to the time of the ice wall formation with the distance between freeze pipes of 0.96 m

4 CONCLUSIONS

This study introduced a bond-based Peridynamic model for simulating coupled heat transfer and water flow with phase change in soils subjected to artificial ground freezing (AGF). The model effectively captures the development of ice walls in coarse-grained soils, even without assuming a transition zone between frozen and unfrozen states - a common limitation of conventional approaches. It is particularly suited for conditions involving high-velocity groundwater flow, where traditional brine freezing is ineffective and expendable refrigerants such as liquid nitrogen or solid carbon dioxide are required.

The model was further applied to evaluate the influence of freeze pipe configuration and geometry under varying seepage velocities. The results demonstrate that both freeze pipe diameter and spacing significantly affect the feasibility and efficiency of ice wall formation, and that expendable refrigerants substantially extend the operational range of AGF in challenging hydrogeological conditions.

The results of this study provide several practical recommendations. Conventional brine freezing should be used only when seepage velocities are low, not exceeding about 0.3 m/day, while SCD and LN freezing remain effective at considerably higher velocities, up to about $v_{al}^{\mathrm{SCD}} \approx 1.4$ m/day and $v_{al}^{\mathrm{LN}} \approx 3.0$ m/day respectively. Where more than one method is feasible, the selection should be guided by an economic comparison. The SCD freezing is generally more cost effective for small frozen volumes. When comparing ice wall delivery times for expendable refrigerant systems, the installation time of the freezing plant must also be considered, as it may be comparable to the freezing time itself. Larger pipe diameters are justified only under high seepage, while smaller diameters remain more economical at low velocities because of reduced drilling requirements. Increased spacing between freeze pipes is appropriate only for LN or SCD systems under seepage, whereas brine freezing requires relatively short spacing even at modest groundwater velocities to ensure reliable ice wall formation.

Overall, the proposed model provides a reliable tool for the engineering design of artificial ground freezing systems, enabling cost-effective and technically robust solutions across a wide range of geological settings and freezing methods.

5 ACKNOWLEDGEMENTS

The authors gratefully acknowledge the financial support provided to P. Nikolaev through a Presidential Doctoral Scholarship Award (PDS Award) from the University of Manchester. A. P. Jivkov also acknowledges funding from the Engineering and Physical Sciences Research Council, UK (EPSRC), under grant EP/N026136/1.

6 REFERENCES

Alzoubi, M.A., Xu, M., Hassani, F.P., Poncet, S. and Sasmito, A.P., 2020. Artificial ground freezing: A review of thermal and hydraulic aspects. *Tunnelling and Underground Space Technology*, 104, p.103534.

Andersland, O.B. and Ladanyi, B., 2004. *Frozen ground engineering*. John Wiley & Sons.

Harris, J.S., 1995. *Ground freezing in practice*. Thomas Telford Ltd.

Madenci, E. and Oterkus, E., 2014. *Peridynamic Theory and Its Applications*. *Peridynamic Theory and Its Applications*, New York, NY: Springer New York.

Nikolaev, P., Jivkov, A.P., Margetts, L. and Sedighi, M., 2023. Non-Local Formulation of Heat Transfer with Phase Change in Domains with Spherical and Axial Symmetries. *Journal of Peridynamics and Nonlocal Modeling*.

Nikolaev, P., Jivkov, A.P., Margetts, L. and Sedighi, M., 2024. Modelling artificial ground freezing subjected to high velocity seepage. *International Journal of Heat and Mass Transfer*, 221, p.125084.

Nikolaev, P., Jivkov, A.P., Sedighi, M., 2025. Artificial ground freezing by solid carbon dioxide—Analysis of controlling factors on ice-wall formation. *Transportation Geotechnics*, 55, p.101691.

Nikolaev, P., Sedighi, M., Jivkov, A.P. and Margetts, L., 2022a. Analysis of heat transfer and water flow with phase change in saturated porous media by bond-based peridynamics. *International Journal of Heat and Mass Transfer*, 185, p.122327.

Nikolaev, P., Sedighi, M., Rajabi, H. and Pankratenko, A., 2022b. Artificial ground freezing by solid carbon dioxide – Analysis of thermal performance. *Tunnelling and Underground Space Technology*, 130, p.104741.